Effect of Stress History on Strength of Cohesive Soils

W. H. PERLOFF, JR., and J. O. OSTERBERG
Respectively, Assistant Professor of Civil Engineering, Ohio State University, and Professor of Civil Engineering, Northwestern University

The purpose of this investigation was to determine, on a behavioral basis, the effect of stress history on the undrained triaxial compressive strength of cohesive soils.

A semitheoretical analysis of the variables affecting shear strength indicates that the undrained shear strength of a given cohesive soil tested at a constant strain rate is a function of the over-consolidation ratio. The effective stresses need not be considered because they are functions of the over-consolidation ratio.

Consolidated undrained triaxial compression tests with measured pore water pressures were performed on remolded clay specimens with varied stress histories. By use of curve-fitting procedures an explicit relationship was found between the strength parameter (the maximum stress difference divided by the consolidation pressure) and the over-consolidation ratio. A similar relationship was found between it and the Skempton pore pressure parameter at failure. Published data from several other investigators for undrained triaxial compression tests on remolded and sedimented soils and undrained extension tests on a remolded soil were found to fit the equations developed.

• SINCE COULOMB (4) presented his empirical equation for the shear strength of cohesive soils, research efforts have been directed toward expressing strength in an explicit form, including as many variables as possible. Coulomb's empirical equation was first modified to consider effective stresses (23) and later the effect of stress history (8, 10). The Coulomb-Hvorslev equation has gained general acceptance, and the validity of the Hvorslev parameters has been demonstrated by many investigators (3, 5). However, the applicability of these parameters in practice is limited by the difficulty of obtaining accurate pore pressure measurements in the zone of failure and by the number of tests that must be performed to evaluate them.

The use of effective stress analysis is not necessary if the shear strength can be expressed in terms of parameters to which effective stresses, or pore water pressures, are also related. In the following sections, such parameters are shown to exist.

Notation.—The symbols used herein are defined where they first appear and for convenience are listed alphabetically in the Appendix.

SEMITHEORETICAL ANALYSIS

Limitations

The analysis is subject to the following limitations and applies only to the following cases:

Paper sponsored by Committee on Stress Distribution in Earth Masses.

1. The analysis applies for an individual saturated clay soil. Different soils will give different values of the material constants.
2. The results are valid only for a single type of test, that is, a consolidated undrained triaxial compression test, where failure is induced by increasing the axial stress while the lateral stress is held constant. For other types of tests, where the boundary stress and strain conditions are changed, different results could be expected. These are likely, however, to be susceptible to this same type of analysis.
3. All specimens tested must have the same initial conditions, such as water content and structure.

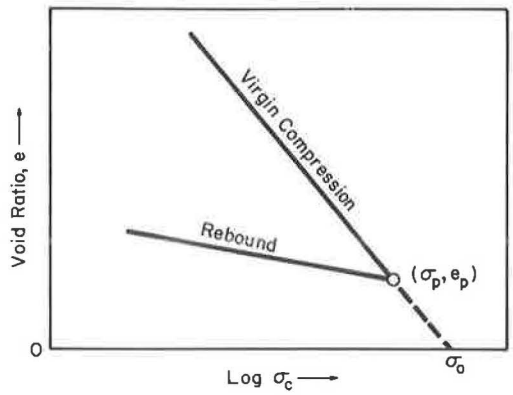

Figure 1. Idealized equilibrium void ratio-pressure relationship.

Assumptions

The assumptions required for the following discussion are:

1. The individual soil particles are incompressible under the magnitude of stresses imposed. This assumption appears reasonable because, according to Skempton and Bishop (21), the cubical compressibility of soil grains is approximately 1×10^{-8} sq cm per kg, whereas that for water is approximately 2.4×10^{-7} sq cm per kg. Thus, water is approximately 24 times more compressible than the soil grains.
2. The compressibility or bulk modulus of water is constant over the range of stresses encountered. Actually, the compressibility of water varies from approximately 2.4×10^{-7} to 2.3×10^{-7} sq cm per kg as the pressure increases from 1 to 10 kg per sq cm. Thus, the compressibility of water varies by about 4 percent over a range of pressures larger than is generally observed in a triaxial compression test on a clay soil.
3. Equilibrium is reached after consolidation under a constant isotropic pressure, and a plot of the equilibrium void ratio, e, vs the consolidation pressure, σ_c, will be a unique curve for a particular soil with given initial conditions. It has been suggested that this assumption will be valid for a great many clays (21, 22, 24). It is not known if soils exhibiting significant secondary compression under isotropic pressures will reach equilibrium. The relative amounts of secondary and primary consolidation in these soils will depend upon the pressure increment ratio, $\Delta P/P_o$ (22, 25). However, Wahls (25) has shown that, for one-dimensional consolidation tests on a soil exhibiting large secondary compression, a unique void ratio-pressure curve can be constructed for the primary consolidation portion and that this curve is independent of $\Delta P/P_o$.
4. The virgin compression curve and the rebound curves on a semilogarithmic plot of void ratio vs pressure can be represented by straight lines (Fig. 1). Furthermore, the slopes of all rebound curves will be the same. Taylor (22) and Terzaghi and Peck (24) suggest that these are reasonable approximations for the majority of cohesive soils. Experimental results from Taylor, Henkel (7), and this paper reinforce this view. Although there is some disagreement about the constancy of the rebound slopes, this assumption appears to be a valid approximation.

FACTORS AFFECTING SHEAR STRENGTH

The Coulomb-Hvorslev equation modified for the triaxial compression test (21) is

$$\frac{\sigma_1 - \sigma_3}{2} = c_e \frac{\cos \varphi_e'}{1 - \sin \varphi_e'} + \sigma_3' \frac{\sin \varphi_e'}{1 - \sin \varphi_e'} \qquad (1)$$

in which $\sigma_1 - \sigma_3$ is the principal stress difference at failure, c_e is the effective cohe-

sion, φ_e' is the effective angle of internal friction, and σ_3' is the effective minor principal stress at failure. Gibson (5) and Bjerrum (3) have demonstrated that, for limitations 1, 2, 3, and a constant strain rate, φ_e' is a soil constant, independent of the void ratio.

For a standard consolidated undrained triaxial compression test

$$\sigma_3 = \sigma_c;\ \sigma_3' = \sigma_c = u_f \tag{2}$$

in which u_f is the pore water pressure at failure. Substituting Eq. 2 into Eq. 1 and making use of the fact that at a constant strain rate, φ_e' is a material constant, Eq. 1 becomes

$$\sigma_1 - \sigma_3 = K_1 c_e + K_2 (\sigma_c - u_f) \tag{3}$$

in which $K_1 = 2 \cos \varphi_e'/(1 - \sin \varphi_e')$ and $K_2 = 2 \sin \varphi_e'/(1 - \sin \varphi_e')$ are soil constants for a constant rate of strain.

Terzaghi (23) and Hvorslev (8, 10) have shown that c_e is a function of the void ratio. Bjerrum and Hvorslev (10) further demonstrated that, for a constant strain rate, there is a linear relationship between the effective cohesion and the equivalent consolidation pressure:

$$c_e = K_3 \sigma_e' \tag{4}$$

in which K_3 is the slope of the linear relationship and σ_e' is the equivalent consolidation pressure. This pressure, corresponding to any e, is the consolidation pressure for a point on the virgin branch of the void ratio-pressure curve with the ordinate e.

Figure 1 shows that the void ratio at any point on the virgin branch of the idealized curve is (assumption 4)

$$e = -C_c \log \left(\frac{\sigma_e'}{\sigma_o}\right) \tag{5}$$

in which C_c is the absolute value of the slope of the virgin curve on a semilogarithmic plot ($C_c = |\Delta e/\Delta \log \sigma|$) and σ_o is the theoretical pressure required to produce a void ratio equal to zero. Rearranging Eq. 5 and solving for the logarithm of σ_e' gives

$$\log \sigma_e' = \log \sigma_o - \frac{1}{C_c} e \tag{6}$$

Substituting Eq. 6 into the logarithm of Eq. 4 yields

$$\log c_e = \log c_z - \frac{1}{C_c} e \tag{7}$$

in which $c_z = K_3 \sigma_o$ is the theoretical effective cohesion at zero void ratio. For limitations 1, 2, 3 and a constant strain rate, c_z will be a material constant (3, 10).

Referring again to the idealized void-ratio pressure relationships (Fig. 1), the void ratio on any portion of the curve can be expressed as (assumption 4)

$$e = -C_c \log \left(\frac{\sigma_p}{\sigma_o}\right) + C_e \log \left(\frac{\sigma_p}{\sigma_c}\right) \tag{8}$$

in which C_e is the absolute value of the slope of the rebound curve on a semilogarithmic plot ($C_e = |\Delta e/\Delta \log \sigma|$), σ_p is the maximum pressure to which the soil has been subjected, and σ_c is the present consolidation pressure producing e. For a normally consolidated specimen, $\sigma_c = \sigma_p$ and the term involving C_e becomes zero (Eq. 5). Eqs. 5 and 8 pertain to equilibrium conditions of the consolidation process and are not related to the rate at which the strength is tested.

Substituting Eq. 8 into Eq. 7 gives

$$\log c_e = \log c_z + \log \left(\frac{\sigma_p}{\sigma_o}\right) + K_4 \log \left(\frac{\sigma_p}{\sigma_c}\right) \tag{9}$$

in which $K_4 = -C_e/C_c$. As a consequence of assumptions 3 and 4, σ_o and K_4 are materi-

al constants. Eq. 9 can be rewritten

$$c_e = \frac{c_z}{\sigma_o} \sigma_p \left(\frac{\sigma_p}{\sigma_c}\right) K_4 \tag{10}$$

Substituting Eq. 10 into Eq. 3 leads to

$$\sigma_1 - \sigma_3 = K_5 \sigma_p \left(\frac{\sigma_p}{\sigma_c}\right) K_4 + K_2 (\sigma_c - u_f) \tag{11}$$

in which $K_5 = K_1 c_z/\sigma_o$, $K_1 = 2 \cos \varphi_e'/(1 - \sin \varphi_e')$, and $K_2 = 2 \sin \varphi_e'/(1 - \sin \varphi_e')$. K_5 and K_2 are material constants when strength is tested at a constant strain rate and $K_4 = -C_e/C_c$ is a material constant independent of the rate of strain.

Eq. 11 shows that, for a constant strain rate, the shearing resistance is a function of several variables, including the pore water pressure at failure, u_f, and, therefore, it is necessary to determine the variables affecting u_f.

Factors Affecting Pore Water Pressure

The development in the following section is a modification of that presented by Skempton and Bishop (21).

If a saturated clay specimen is not permitted to drain, a change in principal stresses of $\Delta\sigma_1$, $\Delta\sigma_2$, $\Delta\sigma_3$ will cause a change in the volume of the specimen. As a consequence of assumption 1, this will be due entirely to a change in volume of the pore spaces. Resistance will come from both phases of the soil-water system: the soil skeleton and the water in the pore spaces.

Resistance Due to Pore Water.—The volume compressibility or bulk modulus of the pore water is defined as

$$C_w = -\frac{1}{V_w} \frac{\Delta V_w}{\Delta u} \tag{12}$$

in which V_w is the initial volume and ΔV_w the change in volume of the water, and Δu is the change in pore water pressure (compression positive). Hence, the pore water pressure is related to the undrained volume change of the specimen in the following way (assumption 1):

$$\Delta V = -V \frac{e}{1 + e} C_w \Delta u \tag{13}$$

in which ΔV is the change of volume of the specimen, V is the total volume of the specimen, $Ve/(1 + e)$ is the volume of the pore water, and C_w is the compressibility of the pore water. The relationship between ΔV and Δu is independent of the stress history or the rate at which the strength is tested (assumptions 2 and 3).

Resistance Due to Soil Skeleton.—To consider the resistance offered to volume change by the soil skeleton, certain quantities involved in this process must be defined: the effective stresses, the compressibility of the soil skeleton, and the "A" factor.

For a triaxial compression test, the changes in the effective principal stresses induced in the soil skeleton are

$$\left.\begin{aligned} \Delta\sigma_1' &= \Delta\sigma_1 - \Delta u \\ \Delta\sigma_2' &= \Delta\sigma_3' - \Delta\sigma_3 - \Delta u \end{aligned}\right\} \tag{14}$$

in which $\Delta\sigma_1'$, $\Delta\sigma_2'$, and $\Delta\sigma_3'$ are, respectively, the changes in the effective major, intermediate, and minor principal stresses and $\Delta\sigma_1$ and $\Delta\sigma_3$ are, respectively, the changes in the total major and minor principal stresses.

The volume compressibility of the soil skeleton under an isotropic pressure is

$$C_s = -\frac{1}{V} \frac{\Delta V'}{\Delta\sigma_a'} \tag{15}$$

in which V is the volume of the specimen, $\Delta V'$ is the change in the volume of the specimen, and $\Delta\sigma_a'$ is the change in effective isotropic stress ($\Delta\sigma_a' = \Delta\sigma_1' = \Delta\sigma_3'$, compression positive).

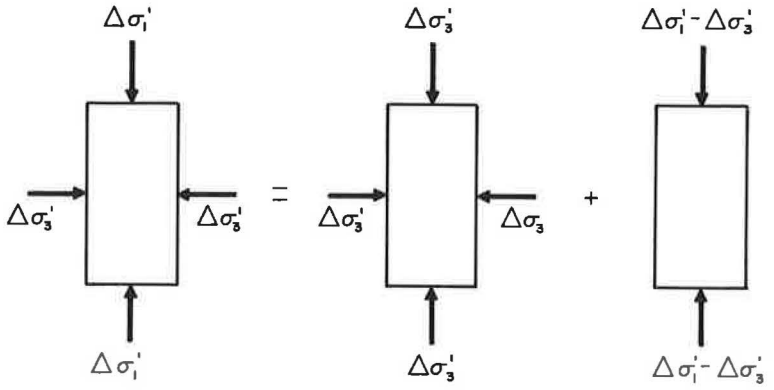

Figure 2. Resolution of general effective stress change into isotropic and uniaxial components.

When dealing with volume change characteristics of the soil skeleton in relation to nonisotropic stress conditions, the role of dilatancy must be considered. Dilatancy is defined as the property of volume change as a consequence of shear distortion. Purely elastic and plastic materials are generally considered to be nondilatant; that is, volume change occurs only as a result of isotropic stresses and shear stresses produce only distortion. These materials do exhibit some dilatancy, but it is a second order effect and can be neglected when strains are small (18).

Soils, in general, do exhibit significant dilatant properties (18, 21, 24). In attempting to express this effect explicity, it is most convenient to think in terms of a uniaxial stress change, rather than a change in the shear stresses (21), because it is the uniaxial stress change that is usually measured in the triaxial compression test.

A general change in effective stresses, $\Delta\sigma_1'$ and $\Delta\sigma_3'$ can be resolved into an isotropic stress change, $\Delta\sigma_3'$, and a uniaxial stress change, $\Delta\sigma_1' - \Delta\sigma_3'$ (Fig. 2). Application of $\Delta\sigma_1' - \Delta\sigma_3'$ will produce a volume change, $\Delta V''$, which can, in principle, be measured. The value of $\Delta V''$ may depend on the magnitude of $\Delta\sigma_1' - \Delta\sigma_3'$ or the manner in which it is applied. There will be some isotropic stress, $\Delta\sigma_m'$, which, if applied in place of $\Delta\sigma_1' - \Delta\sigma_3'$, will produce the same $\Delta V''$. These two stresses can be related in the following way:

$$\Delta\sigma_m' = A\,(\Delta\sigma_1' - \Delta\sigma_3') \tag{16}$$

in which $\Delta\sigma_1' - \Delta\sigma_3'$ is a change in uniaxial stress, $\Delta\sigma_m'$ is the change in isotropic stress that will produce the same volume change as $\Delta\sigma_1' - \Delta\sigma_3'$, and A is a dimensionless parameter representing the relationship between the compressibility of the soil skeleton under a uniaxial stress change and the compressibility under an isotropic stress change. Because $\Delta V''$ may depend upon the value of $\Delta\sigma_1' - \Delta\sigma_3'$ and the manner in which it is applied, A may also depend upon these factors. For an elastic material where strains are small (nondilatant), $A = \frac{1}{3}$. For soils, A varies from approximately +1 to -1, depending upon soil type and certain other variables.

With these definitions it is now possible to formulate the relationship between the volume change, ΔV, and the changes in effective stresses, $\Delta\sigma_1' - \Delta\sigma_3'$. Referring to Eq. 15 and Figure 2, the relationship between the isotropic component of stress increase, $\Delta\sigma_3'$, and the volume change connected to it, $\Delta V'$, is

$$\Delta V' = V C_S \Delta\sigma_3' \tag{17}$$

Referring to Eq. 16 and Figure 2, the relationship between the uniaxial component of stress increase, $\Delta\sigma_1' - \Delta\sigma_3'$, and the volume change connected to it, $\Delta V''$ is

$$\Delta V'' = -V C_S A\,(\Delta\sigma_1' - \Delta\sigma_3') \tag{18}$$

The total change in volume, ΔV, will be the sum of that due to the change in isotropic pressure, $\Delta V'$, and that due to the change in uniaxial stress, $\Delta V''$ (assumption 1). Thus:

$$\Delta V = \Delta V' + \Delta V'' \tag{19}$$

or

$$\Delta V = -V C_S \left[\Delta\sigma_3' + A (\Delta\sigma_2' - \Delta\sigma_3') \right] \tag{20}$$

Combined resistance.—As a consequence of assumption 1, the change in volume of the pore water (Eq. 13) must be equal to the change in volume inclosed by the soil skeleton (Eq. 20) or

$$\frac{e}{1 + e} C_W \Delta u = C_S \left[\Delta\sigma_3 - \Delta u + A (\Delta\sigma_1 - \Delta\sigma_3) \right] \tag{21}$$

in which $\Delta\sigma_3 - \Delta u = \Delta\sigma_3'$ and $\Delta\sigma_1 - \Delta\sigma_3' = \Delta\sigma_1' - \Delta\sigma_3'$ (Eq. 14). Rearranging Eq. 21 to solve for Δu yields

$$\Delta u = \frac{1}{1 + \frac{e}{1 + e}\left(\frac{C_W}{C_S}\right)} \left[\Delta\sigma_3 + A (\Delta\sigma_1 - \Delta\sigma_3) \right] \tag{22}$$

There are few published data indicating values for C_S for different soils. However, Skempton and Bishop (21) have shown that C_S is of the same order of magnitude for isotropic as for one-dimensional consolidation, where it is usually denoted by m_V. An examination was made of results from Taylor (22) and unpublished data at Northwestern University for consolidation tests on many soils to determine a probable minimum value for C_S. The minimum value found was between 10 and 1 kg per sq cm pressure on the rebound curve of a Milwaukee clayey silt specimen from 70 ft below ground surface, where C_S and m_V are 0.001 sq cm per kg. Thus, the order of magnitude of C_W/C_S is likely less than $(2.4 \times 10^{-7})/10^{-3}$ or 2.4×10^{-4} (assumption 2). Therefore, to a very close approximation

$$\frac{1}{1 + \frac{e}{1 + e}\left(\frac{C_W}{C_S}\right)} = 1 \tag{23}$$

and Eq. 22 becomes

$$\Delta u = \Delta\sigma_3 + A (\Delta\sigma_1 - \Delta\sigma_3) \tag{24}$$

Eqs. 22 and 24 are two forms of the well-known pore pressure equation for saturated soils (20).

Expressed in terms of the conditions at failure for a consolidated undrained triaxial compression test ($\Delta\sigma_3 = 0$), Eq. 24 becomes

$$u_f = A_f (\sigma_1 - \sigma_3) \tag{25}$$

in which A_f is A at failure. For a constant strain rate A_f varies from approximately +1 to -1, depending on the soil type and stress history (2, 21).

Elimination of Pore Pressure from Strength Determination

Substituting Eq. 25 into Eq. 11 gives

$$\sigma_1 - \sigma_3 = K_5 \sigma_p \left(\frac{\sigma_p}{\sigma_c}\right) K_4 + K_2 \left[\sigma_c - A_f (\sigma_1 - \sigma_3) \right] \tag{26}$$

Rearranging Eq. 26 and solving for $\sigma_1 - \sigma_3$ yields

$$\sigma_1 - \sigma_3 = \frac{K_5}{1 + K_2 A_f} \sigma_p \left(\frac{\sigma_p}{\sigma_c}\right) K_4 + K_2 \sigma_c \tag{27}$$

Expressing a relationship such as Eq. 27 in dimensionless form, considering each dimensionless ratio as a single variable, permits consideration of a fewer number of

variables and simplifies analysis of experimental results. Such a form is obtained by dividing Eq. 27 by σ_c.

$$\frac{\sigma_1 - \sigma_3}{\sigma_c} = \frac{K_5}{1 + K_2 A_f}\left(\frac{\sigma_p}{\sigma_c}\right)(1 + K_4) + K_2 \tag{28}$$

in which $(\sigma_1 - \sigma_3)/\sigma_c$ is called the shear strength parameter, $K_2 = 2 \sin \varphi_e'/(1 - \sin \varphi_e')$, $K_4 = -C_e/C_c$, σ_p/σ_c is the over-consolidation ratio, and $K_5 = 2 c_z \cos \varphi_e'/\sigma_o (1 - \sin \varphi_e')$. K_2 and K_5 are material constants when the strength is tested at a constant strain rate, and K_4 is a material constant independent of strain rate.

Eq. 28 shows that, for a given soil tested at a particular strain rate, and for the other limitations and assumptions stated above

$$\frac{\sigma_1 - \sigma_3}{\sigma_c} = F_1\left(\frac{\sigma_p}{\sigma_c}, A_f\right) \tag{29}$$

There is no presently available way to determine theoretical relationships for A_f in terms of the variables affecting it because of the definition of A_f. The A factor is, in part, a function of the dilatancy of the soil skeleton. This property, related to the structural arrangement of the clay particles, is not yet well understood, because quantitative description of the changes in structural arrangement in response to stress changes is still lacking. Attempts have been made in this direction (9, 10, 14, 16, 17), but the available information is still quite general. However, it has been shown experimentally (2, 7, 16) that, for Limitations 1, 2, 3 and a constant strain rate, A_f depends only on σ_p/σ_c. Thus, from these investigations, for a constant strain rate

$$A_f = F_2\left(\frac{\sigma_p}{\sigma_c}\right) \tag{30}$$

Substituting Eq. 30 into Eq. 29 gives

$$\frac{\sigma_1 - \sigma_3}{\sigma_c} = F_3\left(\frac{\sigma_p}{\sigma_c}\right) \tag{31}$$

Eq. 31 shows that for the assumptions and limitations stated above, and a constant strain rate, the shear strength parameter for a cohesive soil is a function of the over-consolidation ratio. The strength can be related to these variables without reference to the effective stresses because, as shown by Eq. 30, A_f and, therefore, the effective stresses, are themselves functions of these same variables.

In the following sections experimental results will be used to determine explicit forms for the functional relationships given in Eqs. 30 and 31.

EXPERIMENTAL ANALYSIS

Laboratory experiments were performed to determine the interrelationship between strength and stress history. These experiments consisted of consolidated undrained triaxial compression tests, at several rates of strain, on a saturated clay soil that had been subjected to various stress histories.

Description of Soil Used

The soil used in this investigation has as its chief constituent the clay mineral illite. It is found in the Goose Lake area of Grundy County, Ill., and is sold under the trade name of "Grundite" by the Illinois Clay Products Company. The origin and properties of this soil have been discussed in some detail (6). The clay is upper Pennsylvanian in age and has been exposed, at the site where it is mined, by erosion of the sediments immediately overlying it. Grim and Bradley have said, "The source of this clay, like that of the other underclays of the Pennsylvanian, is believed to be somewhat weathered surface material from the area enclosing the region of accumulation (6). The classification properties are given in Table 1.

TABLE 1

CLASSIFICATION PROPERTIES OF GRUNDITE

w_L (%)	w_P (%)	I_p (%)	G	Clay Fraction (%) (< 2 μ)
54.5	26.0	28.5	2.74	85

TABLE 2

SPECIMEN DIMENSIONS AND PROPERTIES

Length (cm)	Diameter (cm)	Initial Wt. (gm)	w (%)	Void Ratio
7.60	3.54	134.29 ± 0.57	43.2 ± 0.4	1.183 ± 0.012

Specimen Preparation

The Grundite was received from the Illinois Clay Products Company in dry, powdered form. It was mixed, as received, with distilled water to a water content of approximately 43 percent, which was as close to the liquid limit as the soil could be molded. The moist clay was thoroughly mixed by hand and by a mechanical mixer. It was then passed through a "Vac-Aire" sample extruder several times to insure uniform moisture distribution. This equipment, designed for the extrusion of clay specimens, has been described by Matlock et al. (13). On the third time through the extruder, specimens approximately 4 in. long were cut and immediately covered with six coats of a flexible wax. Waxed specimens were placed on a shelf inside a sealed jar with water in the bottom to maintain 100 percent humidity. The jar was then placed in a humid room. The specimens were cured for approximately 6 wk. During that time, at periodic intervals, specimens were removed and tested in unconfined compression to determine if thixotropic hardening was taking place. No evidence of this was found, because the unconfined strengths of all the specimens tested during the 6-wk period after extrusion were the same within ± 1.5 percent.

Testing Procedure

When the soil was ready for triaxial compression testing, each specimen was stripped of its wax cover, which was sufficiently strong to be easily peeled from the specimen. The specimen was then placed in a miter box with an inside diameter exactly equal to that of the specimen. The specimen was trimmed with a wire saw to the proper length and immediately weighed. Specimen dimensions and properties are given in Table 2. After weighing, the specimen was surrounded by drainage strips (2, pp. 81-82), to facilitate consolidation. The specimen was placed inside a 0.005-in. latex membrane which was then painted with Dow-Corning DC 200 silicone fluid to prevent passage of moisture from the soil or glycerine from the chamber into the soil. A second membrane was placed around the first one. The specimen was then mounted in the triaxial compression chamber on a saturated porous stone connected to a pipette open to the atmosphere outside the chamber. The membranes were sealed to the pedestal and loading cap with a layer of Dow-Corning silicone grease and held in place by rubber bands.

The triaxial chamber was filled with glycerine, and the desired consolidation pressure was applied to the glycerine by air pressure. Readings of the water level in the pipette indicated the degree to which consolidation had progressed. One hundred percent consolidation was found to occur in approximately 24 hr when filter strips were

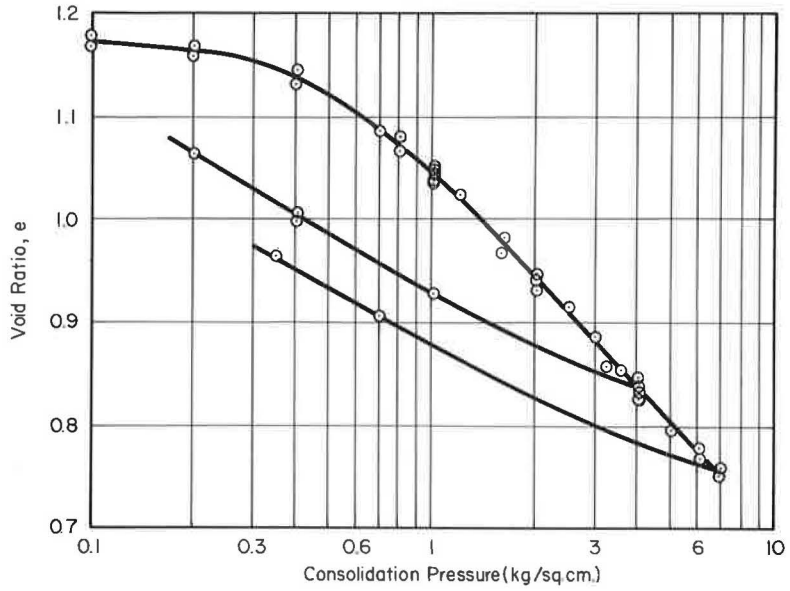

Figure 3. Triaxial consolidation results for Grundite.

used. Wahls (25) showed the importance of the pressure increment ratio, $\Delta P/P_o$, in one-dimensional consolidation tests on a soil exhibiting large secondary compression. However, Grundite exhibited no such secondary compression in triaxial consolidation and, therefore, various pressure increment ratios were chosen by convenience.

A specific over-consolidation ratio, σ_p/σ_c, was obtained by consolidating a specimen under a pressure, σ_p, higher than the preconsolidation pressure induced by the extrusion process (approximately 0.6 kg per sq cm) and then rebounding the specimen under a pressure, σ_c, which gave the desired σ_p/σ_c. Results of these consolidation tests (Fig. 3) represent tests on 23 specimens. Some of the tests consisted of a single load increment, some of several increments. There were too many tests to indicate each with a separate symbol, and to avoid confusion, only two of the rebound curves are shown.

When consolidation was completed, the drainage line was closed, pressure was removed from the triaxial chamber, and the glycerine was drained. The specimen was then taken out of the chamber and the rubber membranes and filter strips were removed. The specimen was immediately recovered by either one or two membranes with a layer of silicone fluid between them, depending on the duration of test to be performed. A solid base and cap were placed on the ends of the specimen. A small hole, approximately $\frac{1}{4}$ in. in diameter, was cut in the membrane at mid-height of the specimen and a pore pressure measuring needle (Fig. 4) filled with distilled water was inserted into the specimen. The needle consisted of a brass tube, $\frac{5}{64}$ in. in diameter and about $1\frac{1}{4}$ in. long, with a wall thickness of $\frac{1}{64}$ in. Two holes, approximately $\frac{3}{8}$ in. in length, were filed in the tube wall in the positions shown in Figure 4. The inside of the tube was filled with a rolled 200 mesh screen to prevent clay from entering the holes. The tube was inserted into $\frac{1}{8}$-in. saran tubing and sealed to the tubing with Chrysler epoxy resin. The tubing was connected to a water-filled copper line leading to a null-balance pore pressure measuring device. This particular device was designed at the Norwegian Geotechnical Institute and constructed by Geonor A/S, Oslo, Norway. The design and operation of this device are described in detail by Andresen et al. (1).

After insertion of the pore pressure needle, the specimen was mounted on the testing frame and the hole in the membrane around the needle was sealed with a liquid rubber compound. The triaxial chamber was placed over the specimen, glycerine was introduced to fill the chamber, and the desired chamber pressure was applied. The solid

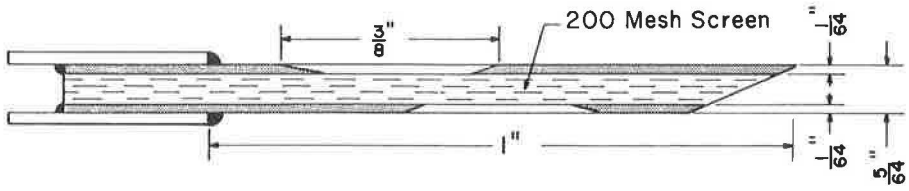

Figure 4. Sketch of pore pressure needle.

lucite cap and base of the specimen permitted no drainage. In general, a chamber pressure of 2 kg per sq cm higher than the consolidation pressure for the specimen was used, to induce a back pressure in the pore water and insure that there were no air bubbles in the soil or measuring system. When pore pressure equilibrium had been reached, the test was begun.

The load on the specimen was measured with a steel proving ring. The pore water pressure was measured with a Bourdon gage connected to the pore pressure apparatus. Deflections of the specimen were measured with a standard dial gage with 0.001-in. divisions.

Four series of tests were performed, each at a different rate of strain. Only one of these series is discussed in this paper. The strain rate for this series was 100 percent per hr. Six specimens each at a different over-consolidation ratio were tested at this strain rate.

The manner in which a specimen failed appeared to depend on the chamber pressure. Under low chamber pressures, 3 kg per sq cm and less, failure occurred along a well-defined shear plane. Little or no bulging was apparent. Under high chamber pressures, 5 kg per sq cm and more, specimens failed by bulging. There was no shear plane evident, although the load on the specimen decreased after reaching a maximum. Between 3 and 5 kg per sq cm chamber pressure, failure appeared to be a combination of both types, although the shear plane was not always very distinct. Sometimes, in this intermediate chamber pressure zone, there were many shear planes apparent and all were parallel. When a shear plane occurred, it was generally parallel to the pore pressure needle and tangent to it. This was very likely because the pore pressure needle created stress concentrations in the specimen. All shear planes were inclined at an angle of approximately 52° to the horizontal. The test results did not appear to be influenced by the mode of failure.

RESULTS

Figure 5 shows the results of the series of tests performed at a strain rate of 100 percent per hr. This figure shows the ratio of the principal stress difference at failure to the consolidation pressure immediately prior to testing $(\sigma_1 - \sigma_3)/\sigma_c$ and the pore pressure parameter at failure $A_f = u_f/(\sigma_1 - \sigma_3)$ as a function of the over-consolidation ratio σ_p/σ_c. In the following discussion, the quantities $(\sigma_1 - \sigma_3)/\sigma_c$ and A_f will always refer to the conditions at failure.

The experimental curves shown in Figure 5 have the appearance of power functions of the form

$$\frac{\sigma_1 - \sigma_3}{\sigma_c} = r\left(\frac{\sigma_p}{\sigma_c}\right)^s + t \tag{32a}$$

and

$$A_f = m\left(\frac{\sigma_p}{\sigma_c}\right)^{-n} + p \tag{32b}$$

where r, s, t and m, n, p are constants for a constant strain rate.

To determine if the experimental data can actually be represented by such equations, curve fitting techniques must be applied.

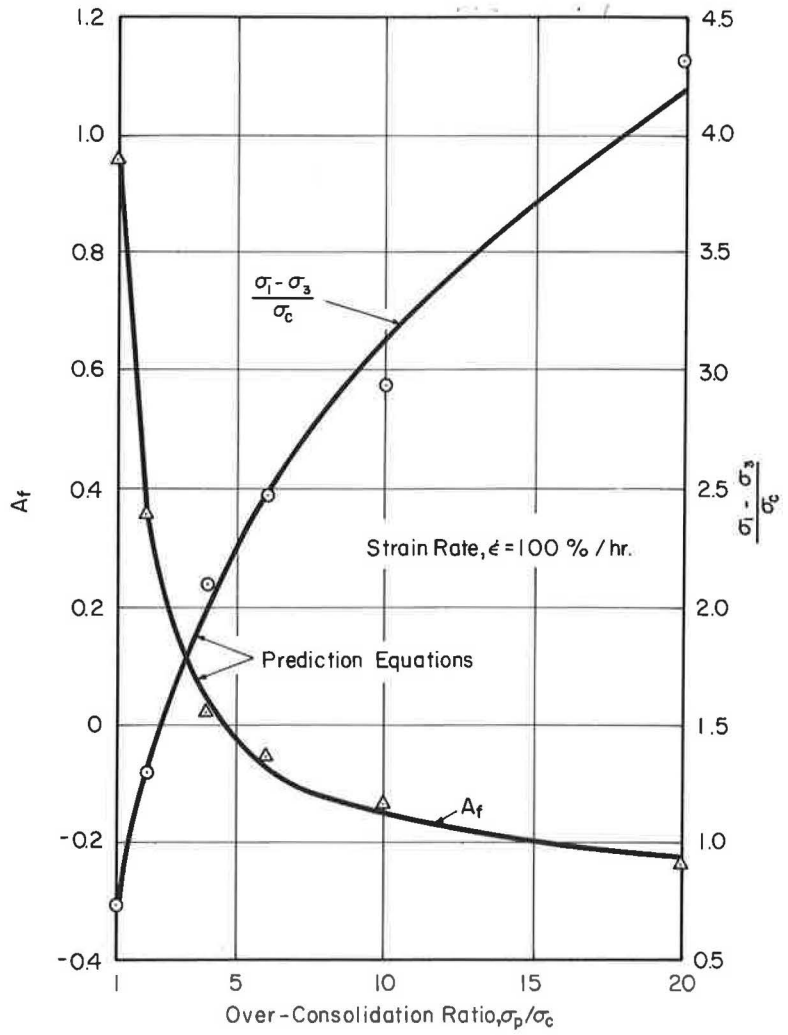

Figure 5. Effect of over-consolidation ratio on failure conditions for Grundite.

Technique and Results of Curve Fitting

If experimental curves are of the form of Eqs. 32a and 32b, then

$$\log\left(\frac{\sigma_1 - \sigma_3}{\sigma_c} - t\right) = \log r + s \log\left(\frac{\sigma_p}{\sigma_c}\right) \tag{33a}$$

and

$$\log\left(A_f - p\right) = \log m - n \log\left(\frac{\sigma_p}{\sigma_c}\right) \tag{33b}$$

Eqs. 33a and 33b are equations of straight lines. Thus, if the experimental data can be described by Eqs. 32a and 32b, they must appear as straight lines when plotted in the form of Eqs. 33a and 33b. Eqs. 33a and 33b are, therefore, test plots of the validity of representing the experimental results by Eqs. 32a and 32b.

However, in order to make the test plots, the constants t and p must be evaluated. Johnson (11, p. 117) suggests a method for calculating mathematically the value of the

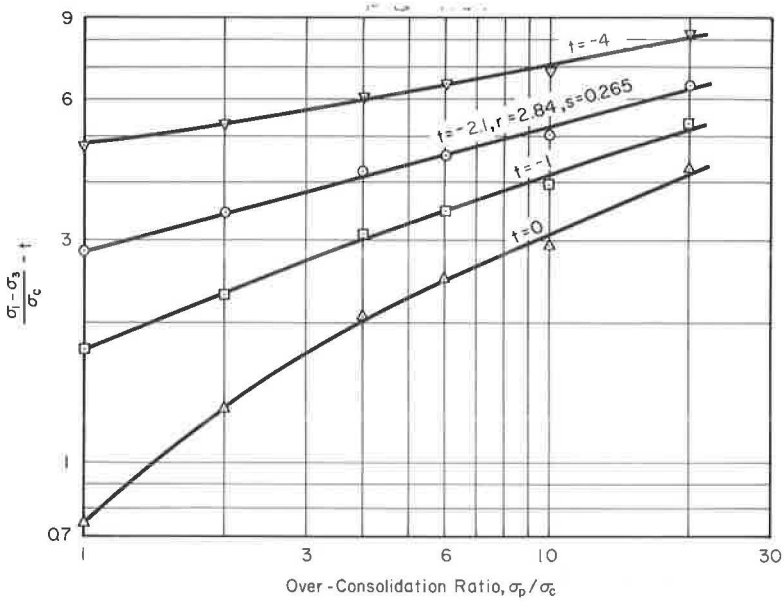

Figure 6. Test plots of strength equation for Grundite clay, ε = 100 percent per hr.

required constants. But because his method involves the use of several actual data points and a certain amount of scatter in the data is common, several trials are generally necessary before the correct values of t and p are found. Therefore, straight trial-and-error procedure is much simpler. Figure 6 illustrates this procedure for the test plot of Eq. 33a with the results of tests at a strain rate of 100 percent per hr. The lowest curve in this figure is a plot of the raw data, t = 0. Because the points do not lie on a straight line on the logarithmic plot, t = 0 will not yield an equation to fit the experimental data. Above this curve, the data are plotted for t = -1.00. This curve is not a straight line, but it is distinctly flatter than the lower curve. The uppermost curve, with t = -4.00, has reversed its curvature, indicating that the absolute value of t is too large. The set of points below this, where t = -2.10, adheres to a straight line. This indicates that the experimental data can be fairly represented by Eq. 33a and, therefore, by Eq. 32a, for t = -2.10. The best straight line through the experimental points on the logarithmic plot was determined by the method of least squares.

The constants r and s are found by substitution in Eq. 32a. When $\sigma_p/\sigma_c = 1$, log $(\sigma_p/\sigma_c) = 0$ and $r = (\sigma_1 - \sigma_3)/\sigma_c - t$. The constant s is the slope of the straight line on the logarithmic plot. Thus, s is equal to the logarithm of the ratio between two values of $(\sigma_1 - \sigma_3)/\sigma_c - t$, which are one cycle apart. Application of these procedures to the straight line curve in Figure 6 for t = -2.10 yields r = 2.84 and s = 0.265.

Figure 7 is a test plot of Eq. 32b for the pore pressure parameter data for the test series discussed previously. Again, it can be seen that the points lie along straight lines, indicating that the experimental data can be represented by Eq. 32b. The numerical values of the constants m, n, p are shown on the test plot. The close fit of Eqs. 32a and 32b to the experimental data can also be seen in Figure 5. The "experimental curves" for $(\sigma_1 - \sigma_3)/\sigma_c$ and A_f vs σ_p/σ_c are, in fact, plots of Eqs. 32a and 32b with the appropriate constants found from Figures 6 and 7.

RESULTS FROM OTHER INVESTIGATIONS

Jurgenson (12) and Rutledge (19) investigated the shear strength of cohesive soils in terms of external variables for the simplest case, that is, normally consolidated soil, in which the strain rate was held constant. They both found that $(\sigma_1 - \sigma_3)/\sigma_c$

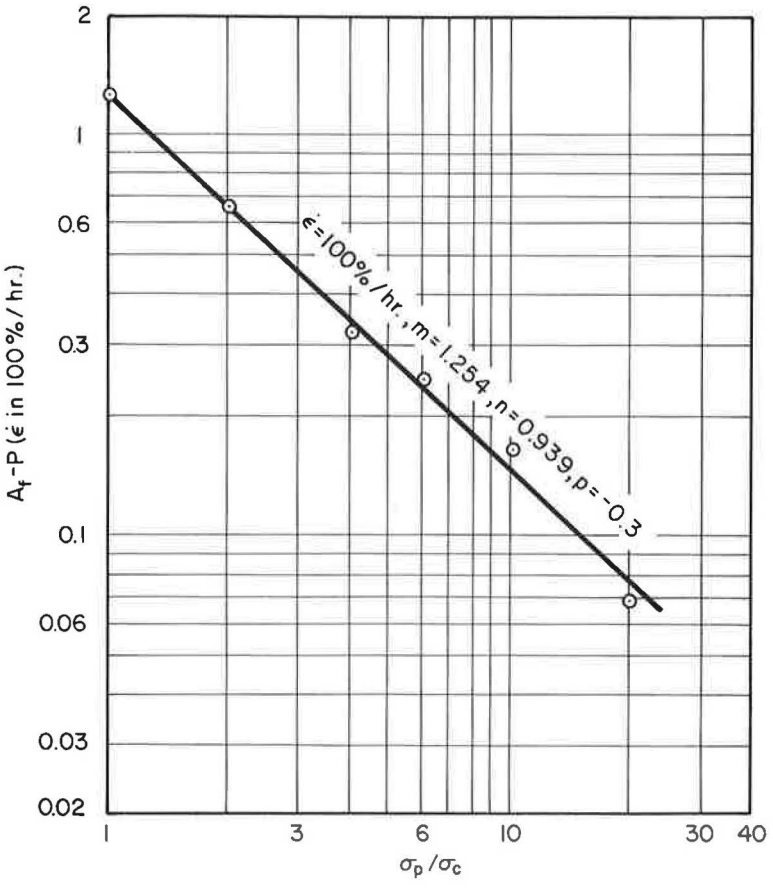

Figure 7. Test plot of pore pressure parameter equation for Grundite.

equaled a constant. Their work is verified by Eq. 32a which, for a normally consolidated soil (σ_p/σ_c = 1) reduces to

$$\frac{\sigma_1 - \sigma_3}{\sigma_c} r + t = \text{constant} \tag{34}$$

They were able to circumvent the use of effective stresses because Eq. 32b and, therefore, the pore pressure, exhibits a similar relationship:

$$A_f = m + p = \text{constant} \tag{35}$$

for σ_p/σ_c = 1.

Henkel (7) and Parry (16) performed series of consolidated drained and undrained triaxial compression and extension tests at a constant strain rate on remolded Weald clay, and consolidated drained and undrained triaxial compression tests on remolded London clay varying the stress history. The tests discussed in the following were consolidated undrained triaxial compression tests in which failure was induced by increasing the axial stress at a constant rate of strain as the lateral stress was held constant. Pore water pressures were measured at the base of the specimens and filter strips were used on the sides of the specimen to reduce pore pressure gradients. The classification properties of the two clays are given in Table 3 (16).

The results of these tests are replotted to arithmetic scales in Figures 8 and 9. The resultant experimental curves, again, have the general shape of power functions of the form of Eqs. 32a and 32b. The data were tested by the method previously outlined to

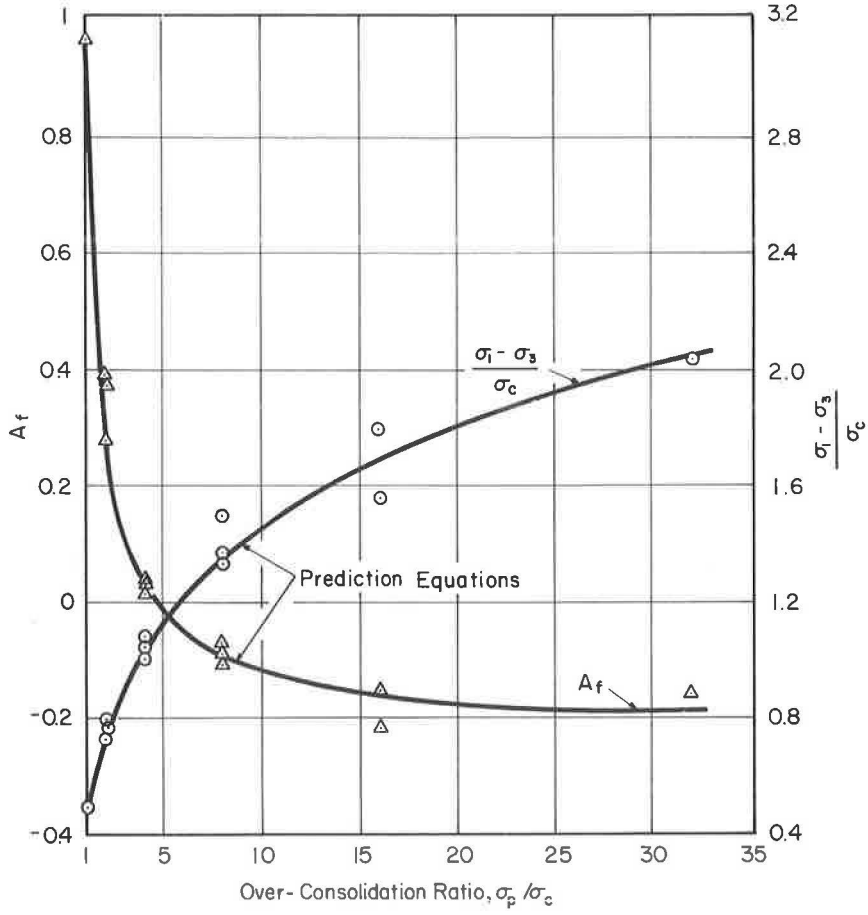

Figure 8. Effect of over-consolidation ratio on failure conditions for London clay (7).

determine if they could be represented by these equations. The test plots are shown in Figures 10 and 11. It is evident from these figures that Eqs. 32a and 32b fairly represent the experimental results. This is further verified in Figures 8 and 9, where the "experimental curves" are, in fact, plots of these equations with the appropriate constants determined in Figures 10 and 11.

TABLE 3

CLASSIFICATION PROPERTIES OF WEALD CLAY AND LONDON CLAY

Type	w_L (%)	w_P (%)	I_p (%)	Clay Fraction (%)
Weald Clay	43	18	25	40
London Clay	78	26	52	50

Olson (15) performed consolidated undrained triaxial compression tests on sedimented and remolded specimens of a calcium illite, varying the stress history. Classification properties of the calcium illite are given in Table 4. These data have been used to plot Figures 12 and 13, which show the effect of over-consolidation on $(\sigma_1 - \sigma_3)/\sigma_c$ and A_f for both sedimented and remolded specimens of calcium illite. The test plots of Eqs. 33a and 33b are shown in Figures 14 and 15. Again, the test plots indicate the validity of Eqs. 32a and 32b for this soil. The "experimental curves" in Figures 12 and 13 are, as before, plots of Eqs. 32a and 32b with the

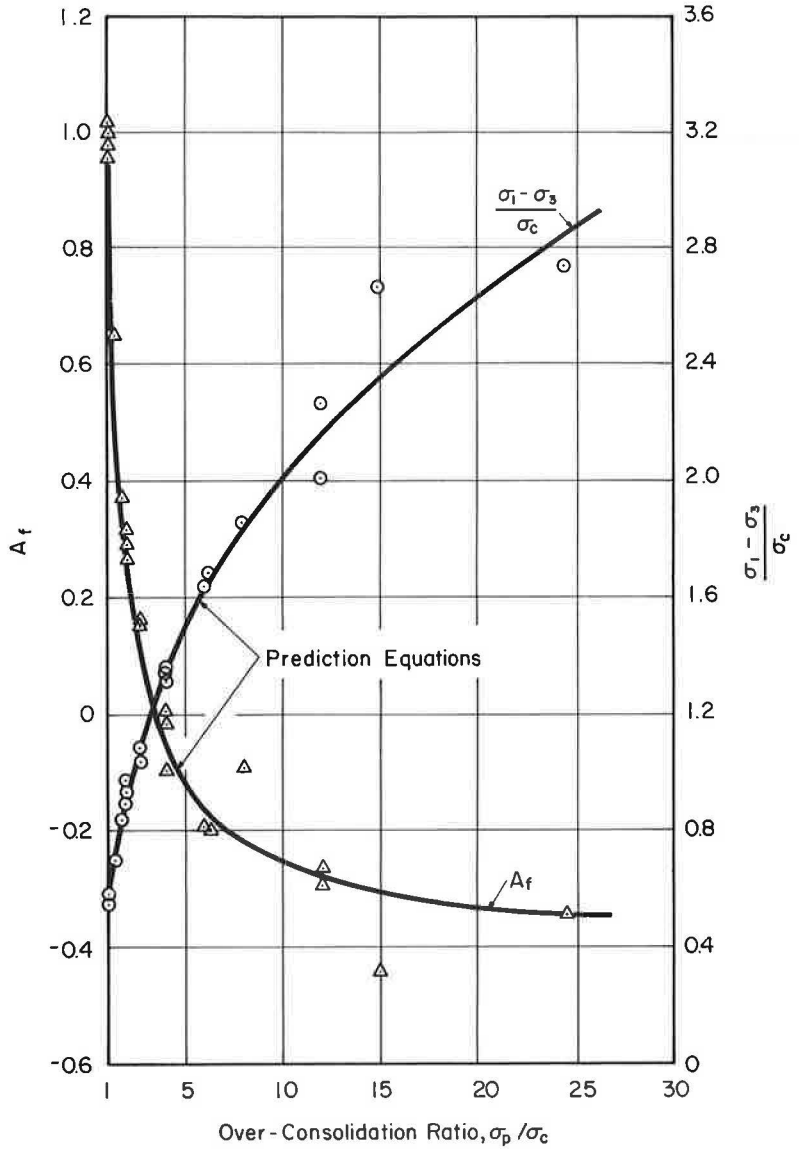

Figure 9. Effect of over-consolidation ratio on failure conditions for Weald clay (16).

constants determined from Figures 14 and 15.

The results of the consolidated undrained extension tests from Parry (16) can also be described by Eqs. 32a and 32b. These results are shown in Figure 16, with the test plots shown in Figures 17 and 18.

TABLE 4

CLASSIFICATION PROPERTIES OF CALCIUM ILLITE

w_L (%)	w_P (%)	I_p (%)	Clay Fraction (%)
85	37	48	100

DISCUSSION OF RESULTS

The relationship of the "constants" previously discussed to the physical properties of soils is not immediately obvious. Although Eq. 32a appears to be of the same form

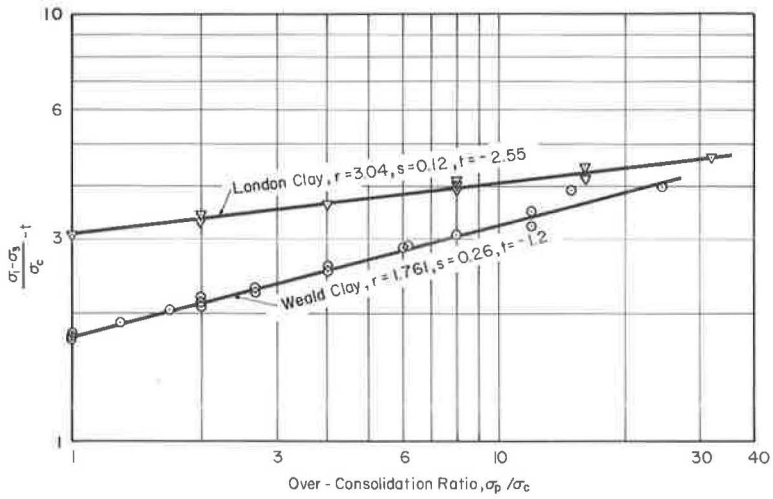

Figure 10. Test plots of strength equation for Weald clay (16) and London clay (7).

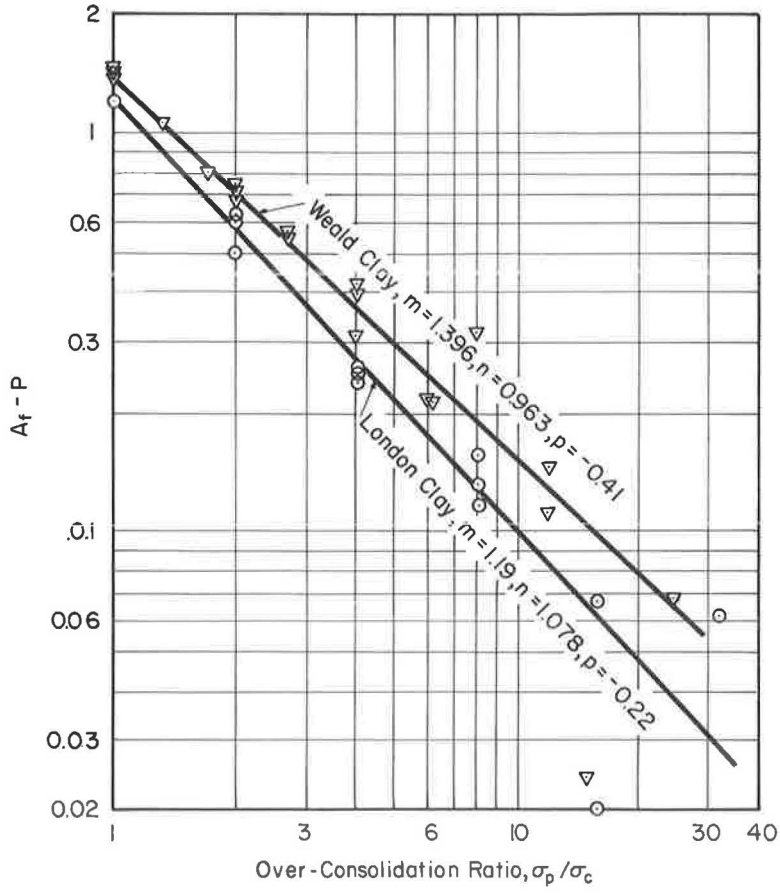

Figure 11. Test plots of pore pressure parameter equation for Weald clay (16) and London clay (7).

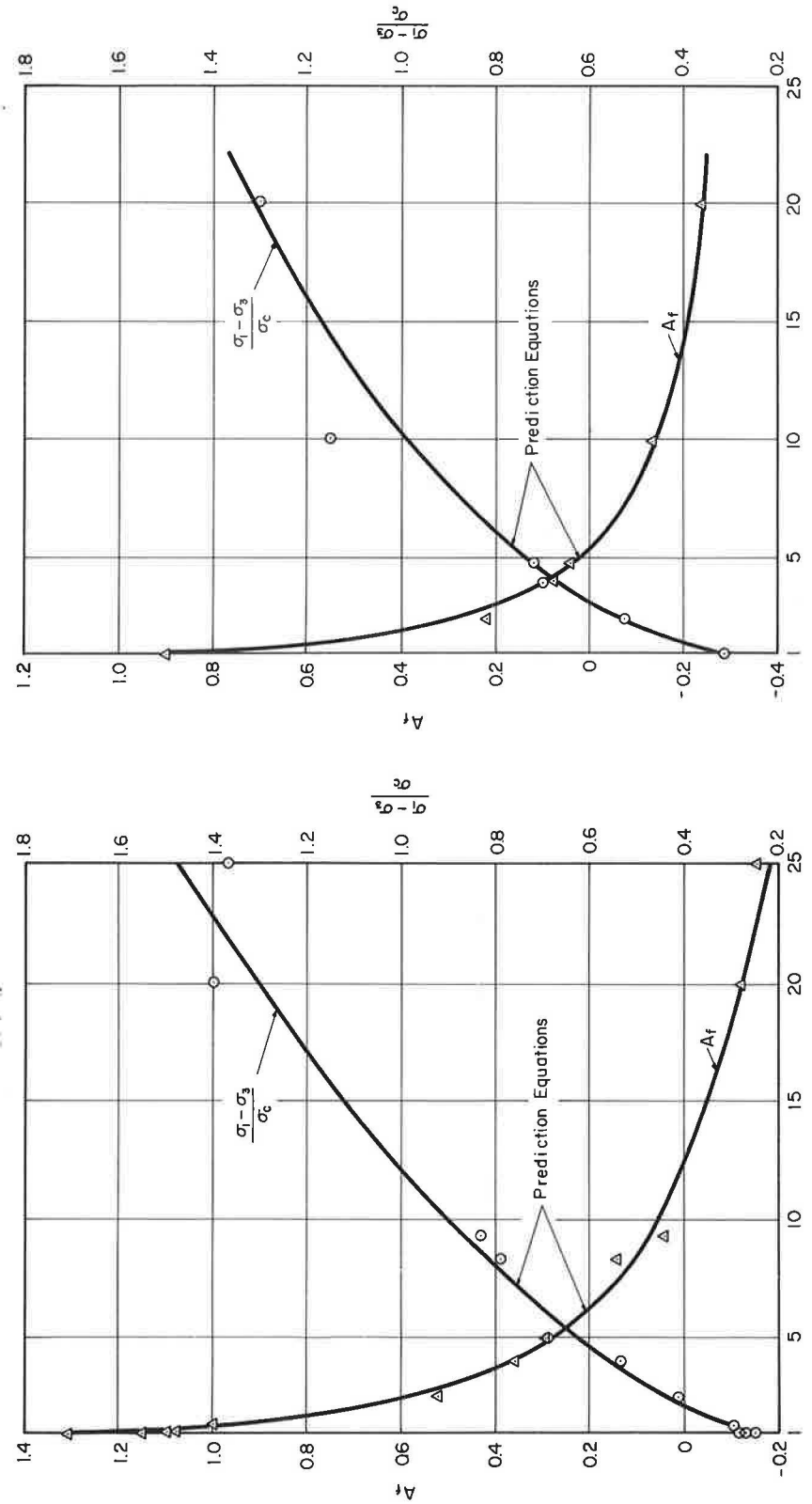

Figure 12. Effect of over-consolidation ratio on failure conditions for sedimented calcium illite (15).

Figure 13. Effect of over-consolidation ratio on failure conditions for remolded calcium illite (15).

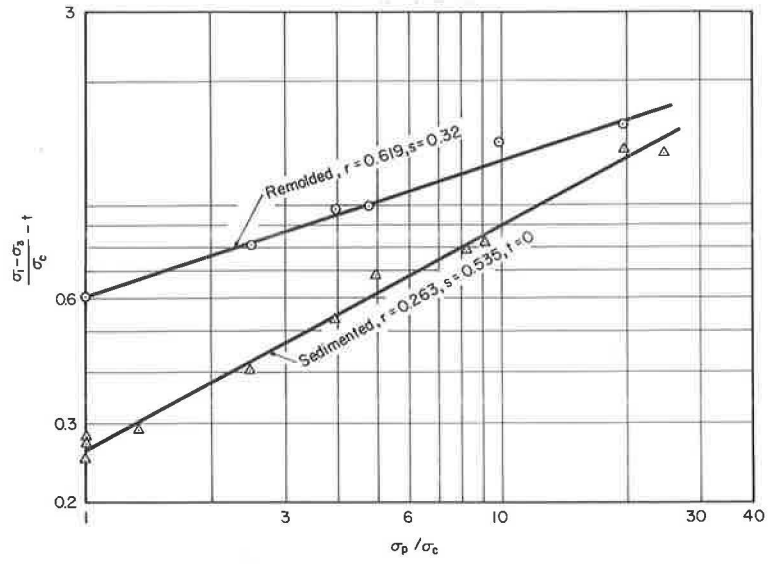

Figure 14. Test plot of strength equation for calcium illite (15).

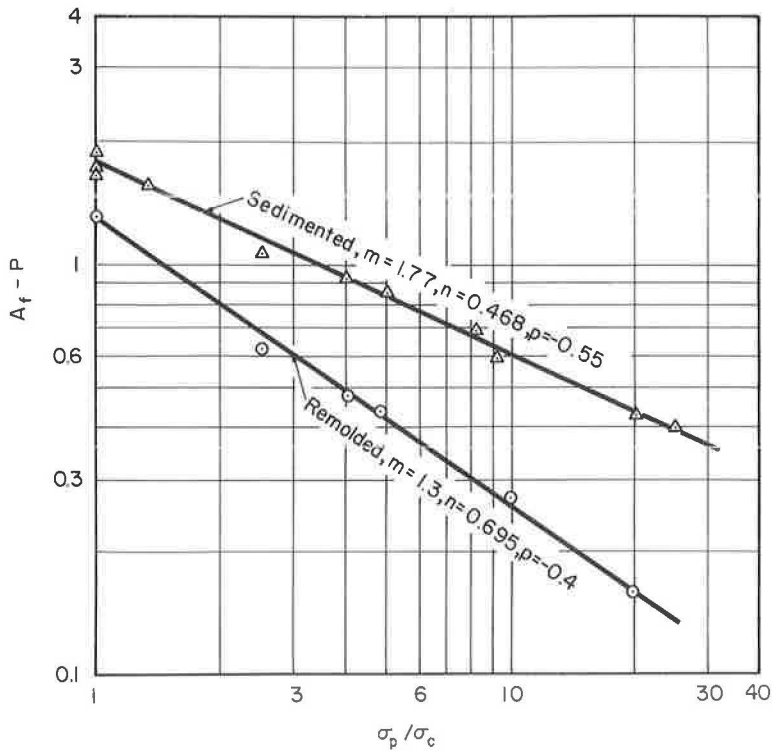

Figure 15. Test plots of pore pressure parameter equation for calcium illite (15).

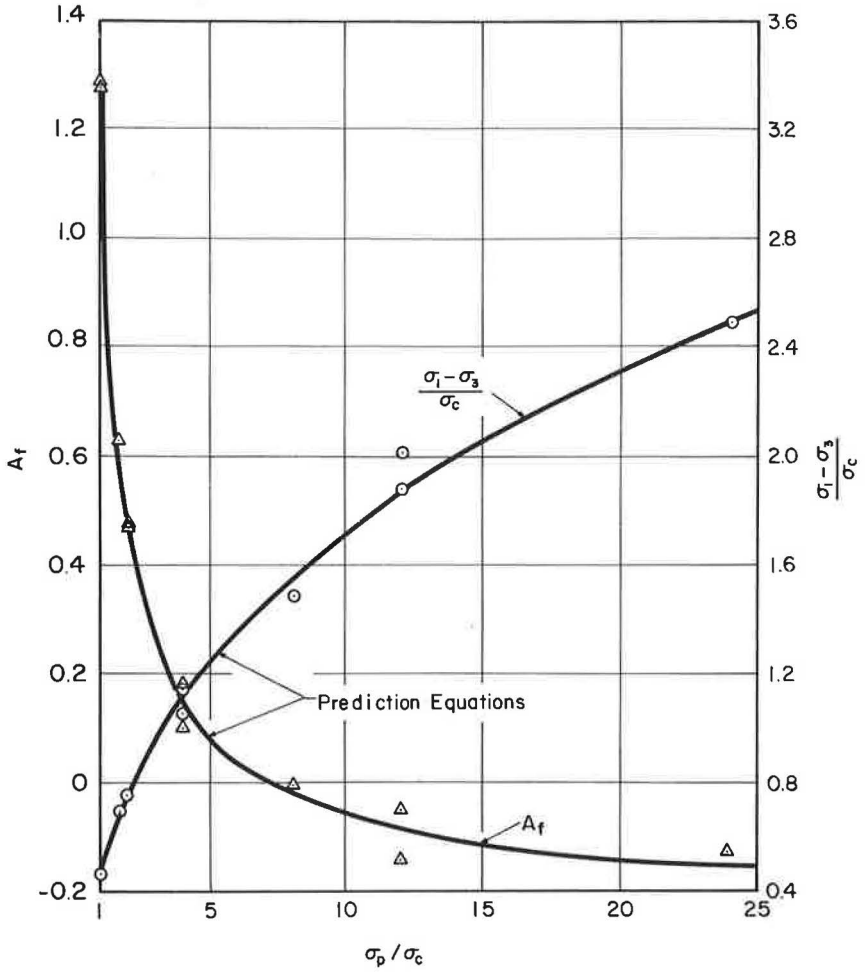

Figure 16. Effect of over-consolidation ratio on failure conditions for extension tests on Weald clay (16).

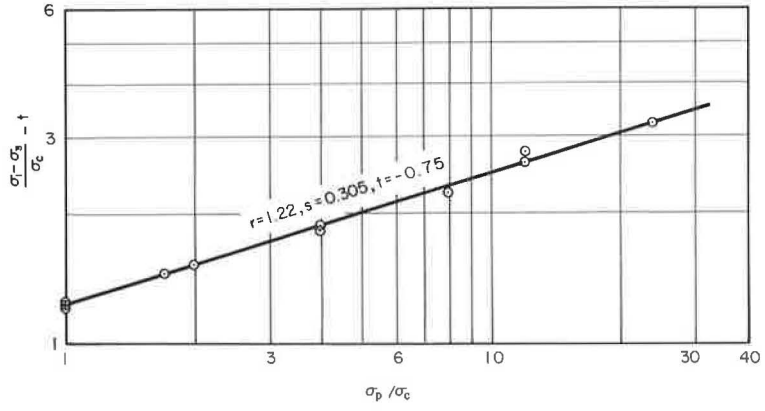

Figure 17. Test plot of strength equation for extension tests on Weald clay (16).

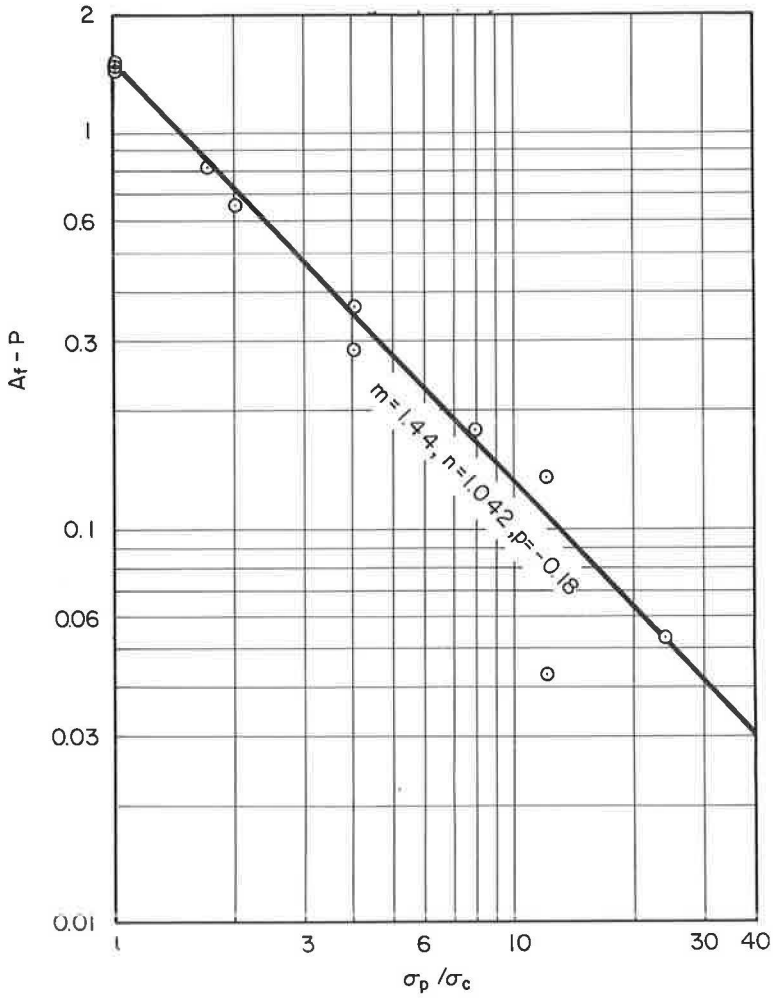

Figure 18. Test plot of pore pressure parameter equation for extension tests on Weald clay (16).

as Eq. 28, this similarity is misleading. Because Eq. 28 contains A_f in the denominator of the first term, A_f may influence the form of a theoretical expression containing A_f as a function of σ_p/σ_c. Thus Eqs. 32a and 28 are not directly comparable. Substitution of Eq. 32b into Eq. 28 to eliminate A_f yields an expression much more complex than Eq. 32a. This is not surprising, because Eqs. 32a and 32b are empirical relationships. The variables involved have been determined on a semitheoretical basis, but the power function form is only suggested by theoretical considerations. Some other function, such as a Fourier series, might be manipulated to produce the same empirical curve. The stress history constant t in Eq. 32a represents the theoretical value of $(\sigma_1 - \sigma_3)/\sigma_c$ when $\sigma_p/\sigma_c = 0$. In practice, of course, it is not possible to test a specimen with an over-consolidation ratio equal to zero, just as it is difficult to conceive of a negative $(\sigma_1 - \sigma_3)/\sigma_c$.

The stress history constant p in Eq. 32b can be shown to have a physical interpretation. As σ_p/σ_c approaches infinity, in Eq. 32b, A_f approaches p. Thus p is the limiting value of A_f as the over-consolidation ratio approaches infinity. In order to verify this experimentally, one test was performed on a specimen consolidated under 2 kg per sq cm and rebounded under zero stress. Thus σ_p/σ_c was equal to infinity. The meas-

ured value of A_f was -0.328, which compared favorably to the value of p = -0.300 found in Figure 7.

These results clearly indicate the applicability of Eqs. 32a and 32b to a variety of soils, tested, undrained, under a variety of stress conditions. The undrained shear strength of these soils at any degree of over-consolidation can be predicted without the use of effective stresses, because for a given soil and a given type of test, the strength and pore pressure parameters at failure are both uniquely related to the over-consolidation ratio.

CONCLUSIONS

Based on the results of this investigation, the following conclusions can be drawn.

1. For the several cohesive soils examined, both remolded and sedimented, when tested in consolidated undrained triaxial compression, an explicit empirical equation can be written relating the shear strength parameter, $(\sigma_1 - \sigma_3)/\sigma_c$, to the over-consolidation ratio, without the use of effective stress analysis. The use of these variables can be justified semitheoretically.
2. The use of effective stress analysis is not necessary because the Skempton pore pressure parameter at failure, and therefore, the effective stresses are also a function of the over-consolidation ratio.
3. Published results from another investigation indicate that the preceding conclusions are also valid for consolidated undrained extension tests on a remolded soil.

ACKNOWLEDGMENT

This research was made possible by a grant from the Advanced Research Projects Agency of the United States Department of Defense administered by the Materials Research Center of Northwestern University.

REFERENCES

1. Andresen, A., Bjerrum, L., Di Biago, E., and Kjaernsli, B., "Triaxial Equipment Developed at the Norwegian Geotechnical Institute." Norwegian Geotechnical Publ. 21 (1957).
2. Bishop, A. W., and Henkel, D. J., "The Measurement of Soil Properties in the Triaxial Test." Edward Arnold, Ltd., London, England (1957).
3. Bjerrum, L., "Theoretical and Experimental Investigations on the Shear Strength of Soils." Norwegian Geotechnical Publ. 5 (1954).
4. Coulomb, C. A., "Essai sur une Application des Regles de Maximis et Minimis à Quelques Problemes de Statique, Relatifs a l' Architecture." Mem. Acad. Sci. (Savants Etrangers), 7:343-382 (1776).
5. Gibson, R. E., "Experimental Determination of the True Cohesion and True Angle of Internal Friction in Clays." Proc. 3rd Internat. Conf. on Soil Mechanics and Foundation Eng., I, pp. 126-130 (1953).
6. Grim, R. E., and Bradley, R. F., "A Unique Clay from the Goose Lake, Illinois Area." Jour. Amer. Ceram. Soc., 22:5 (May, 1939).
7. Henkel, D. J., "Effect of Overconsolidation on Behavior of Clays During Shear." Geotechnique, VI:4 (Dec. 1956).
8. Hvorslev, M. J., "Conditions of Failure for Remolded Cohesive Soil." Proc. 1st Internat. Conf. on Soil Mechanics and Foundation Eng., III:51-53 (1936).
9. Hvorslev, M. J., "The Shearing Resistance of Remolded Cohesive Soils." Proc. U. S. Eng. Dept. Soils and Foundations Conference, Boston (1938).
10. Hvorslev, M. J., "Physical Components of the Shear Strength of Saturated Clays." U. S. Army Engineer Waterways Exp. Sta. Misc. Paper 3-428 (Jan. 1961).
11. Johnson, L. H., "Nomography and Empirical Equations." John Wiley, New York (1952).
12. Jurgenson, L., "The Shearing Resistance of Soils." Jour. Boston Soc. of Civil Eng., XXI:3 (July 1934).
13. Matlock, H., Jr., Fenske, C. W., and Dawson, R. F., "De-aired, Extruded Soil Specimens for Research and for Evaluation of Test Procedures." ASTM Bull. 177 (Oct. 1951).

14. Mitchell, J. K., "The Fabric of Natural Clays and Its Relation to Engineering Properties." Proc. HRB, 35:693-713 (1956).
15. Olson, R. E., "The Shear Strength Properties of Calcium Illite." Geotechnique, XII:1 (March 1962).
16. Parry, R. H. G., "Triaxial Compression and Extension Tests on Remolded Saturated Clay." Geotechnique, X:4 (Dec. 1960).
17. Perloff, W. H., Jr., "The Effect of Stress History and Strain Rate on the Undrained Shear Strength of Cohesive Soils." Ph. D. Dissertation, Northwestern Univ. (June 1962).
18. Reiner, M., "Deformation, Strain and Flow." 2nd Ed., Interscience Publishers, New York (1960).
19. Rutledge, P. C., "Cooperative Triaxial Shear Research Program of the Corps of Engineers." Soil Mechanics Fact Finding Survey, Progr. Rep. U. S. Army Engineer Waterways Exp. Sta. (April 1947).
20. Skempton, A. W., "The Pore Water Coefficients A and B." Geotechnique, IV:4 (Dec. 1954).
21. Skempton, A. W., and Bishop, A. W., "Soils." Chapter X from "Building Materials. Their Elasticity and Inelasticity." Ed., M. Reiner, North Holland Publishing Co., Amsterdam, Holland, pp. 417-482 (1954).
22. Taylor, D. W., "Fundamentals of Soil Mechanics." John Wiley Publishing Co., New York (1948).
23. Terzaghi, K., "The Shearing Resistance of Saturated Soils and the Angle Between the Planes of Shear." Proc. 1st Internat. Conf. on Soil Mechanics and Foundation Eng., I:54-56 (1936).
24. Terzaghi, K., and Peck, R. B., "Soil Mechanics in Engineering Practice." John Wiley Publishing Co., New York (1948).
25. Wahls, H. E., "Primary and Secondary Effects in the Consolidation of Cohesive Soils." Unpubl. Ph. D. Thesis, Northwestern Univ.

Appendix

A = Skempton pore pressure parameter;
A_f = Skempton pore pressure parameter at failure;
C_e = expansion index;
C_c = compression index;
C_s = compressibility of the soil skeleton ($F^{-1}L^2$);
C_w = compressibility of water ($F^{-1}L^2$);
c_e = Hvorslev effective cohesion (FL^{-2});
c_z = theoretical effective cohesion at zero void ratio (FL^{-2});
e = void ratio;
$F_N(x)$ = a function of x;
I_p = plasticity index = $w_L - w_P$;
m = stress history constant for the pore pressure parameter prediction equation;
N = an integer;
n = stress history constant for the pore pressure parameter prediction equation;
p = stress history constant for the pore pressure parameter equation;
$\Delta P/P_o$ = pressure increment ratio for a consolidation test;
r = stress history constant for the strength prediction equation;
s = stress history constant for the strength prediction equation;
t = stress history constant for the strength prediction equation;
Δu = pore pressure change due to a change in principal stresses (FL^{-2});
u_f = pore pressure at failure (FL^{-2});
w = water content;
w_L = liquid limit;
w_P = plastic limit;
ϕ_e' = Hvorslev effective angle of internal friction;
σ_1 = major total principal stress (FL^{-2});
σ_2 = intermediate total principal stress (FL^{-2});

σ_3 = minor total principal stress (FL^{-2});
σ_1' = major effective principal stress (FL^{-2});
σ_2' = intermediate effective principal stress (FL^{-2});
σ_3' = minor effective principal stress (FL^{-2});
$(\sigma_1 - \sigma_3)$, $(\sigma_1' - \sigma_3')$ = principal stress difference (FL^{-2});
σ_c = consolidation pressure immediately prior to strength test (FL^{-2});
σ_e' = Hvorslev equivalent consolidation pressure (FL^{-2});
σ_o = theoretical pressure required to produce zero void ratio (FL^{-2});
σ_p = maximum preconsolidation pressure (FL^{-2}); and
σ_p/σ_c = over-consolidation ratio.